Design Method for Tunable Planar Bandpass Filters With Single-Bias Control and Wide Tunable Frequency Range

Taejun Lim, *Member, IEEE*, Akash Anand, *Member, IEEE*, James Chen, *Member, IEEE*, Xiaoguang Liu, *Senior Member, IEEE*, and Yongshik Lee, *Senior Member, IEEE*

***Abstract*—A design method for a frequency-tunable planar bandpass filter is demonstrated. With the method, all reasonators can be designed with identical capacitances, allowing the filter to be tuned with identical varactors using a single bias control. This allows not only low-cost fabrication, but also a simple structure and design procedure. Moreover, the filter is based on miniaturized transmission lines. Therefore, a wide tuning range is achieved with a small size and outstanding out-of-band response. Most importantly, the method facilitates the design of a filter to vary the fractional bandwidth in a predetermined way as the center frequency is tuned. Thus, a tunable filter can be designed not only to maintain the fractional bandwidth, but also to expand or to reduce the bandwidth as the frequency is tuned. The experimental results of a compact third-order bandpass filter based on CPW lines with a $0.11\lambda_g \times 0.8\lambda_g$ size show a very wide frequency tuning range of 62.8% with a 3-dB fraction bandwidth that remains within 28.65±1.55% and an outstanding spurious suppression of under −40 dB up to as high as $3f_0$.**

***Index Terms*—Electronically tunable filter, varactor-tuned filter, planar filter, single-bias control, wide tuning range.**

I. Introduction

MICROWAVE filters are an essential component of microwave communication systems. Researchers have successfully achieved compact size, wide or multiple passbands, and harmonic suppression [1], [2]. Moreover, the rapid growth of modern wireless communication services presents design challenges to develop filters with advanced performance.

For instance, frequency tunable filters are critical components in future multifunctional systems for communication and sensing applications [3], [4]. These filters can be reconfigured to tune the passband by controlling the resonant conditions of each resonator, generally based on varactor diodes. One of the most difficult design challenges for these tunable filters is to maintain the passband characteristics, for instance the fractional or absolute bandwidth, while the center frequency is tuned. In [5]–[8], microstrip resonators with end-loaded varactors are utilized to compensate for the changes in the coupling coefficients as the frequency is tuned. Although frequency tuning can be achieve relatively easily with varactors, semiconductor varactors often suffer from low quality factor (Q). Alternative techniques for the development of high-Q frequency tunable filters include high-temperature superconducing (HTS) resonators [9] and substrate-integrated resonators [10].

The frequency tuning range is another key performance for frequency tunable filters [11]–[13]. The tuning range of varactor capacitances is a major limiting factor that determines the frequency tuning range. Therefore, various structural modifications have been proposed to maximize the frequency tuning range for a given varactor tuning range, which include microstrip ring resonators [11], [12] and stepped-impedance resonators [13]. In addition, harmonic suppression is also indispensable as the filter is tuned [14]. To satisfy all these requirements, relatively complex structures may be required to control the resonators and/or inter-resonator coupling individually.

This brief presents a design method for a frequency-tunable planar filter based on transmission lines. The reduced lengths of these transmission lines provides a very wide tuning range, small size, and outstanding spurious response. Furthermore, the method allows all resonators to be tuned with the same varactors controlled by a single bias to allow a simple structure, simple design procedure, and low-cost fabrication. More importantly, the method is based on rigorous analysis that takes into account the parasitic inductance of the varactor. Therefore, accurate estimation of the frequency tuning range is possible, in which the bandwidth is maintained, expanded, or reduced as the frequency is tuned. Finally, the filter can be tuned with identical varactors and a single bias, which is a great advantage since it not only simplifies the structure and the design, but also provides low-cost fabrication and less sensitivity to fabrication tolerance [15].

For verification, a 3rd-order Chebyshev bandpass filter having a compact size of $0.11\lambda_g \times 0.8\lambda_g$ at 1.52 GHz is designed

Manuscript received May 18, 2020; accepted June 13, 2020. Date of publication June 24, 2020; date of current version December 21, 2020. This work was supported by the National Research Foundation of Korea (NRF) grant funded by the Korea Government (MSIT) under Grant 2020R1A2C1010251. This brief was recommended by Associate Editor Q. Liu. *(Corresponding author: Yongshik Lee.)*

Taejun Lim and Yongshik Lee are with the Department of Electrical and Electronic Engineering, Yonsei University, Seoul 120-749, South Korea (e-mail: yongshik.lee@yonsei.ac.kr).

Akash Anand and Xiaoguang Liu are with the Department of Electrical and Computer Engineering, University of California at Davis, Davis, CA 95616 USA (e-mail: lxgliu@ucdavis.edu).

James Chen is with the Department of Electrical and Computer Engineering, Stanford University, Stanford, CA 94305 USA.

Color versions of one or more of the figures in this article are available online at https://ieeexplore.ieee.org.

Digital Object Identifier 10.1109/TCSII.2020.3004614

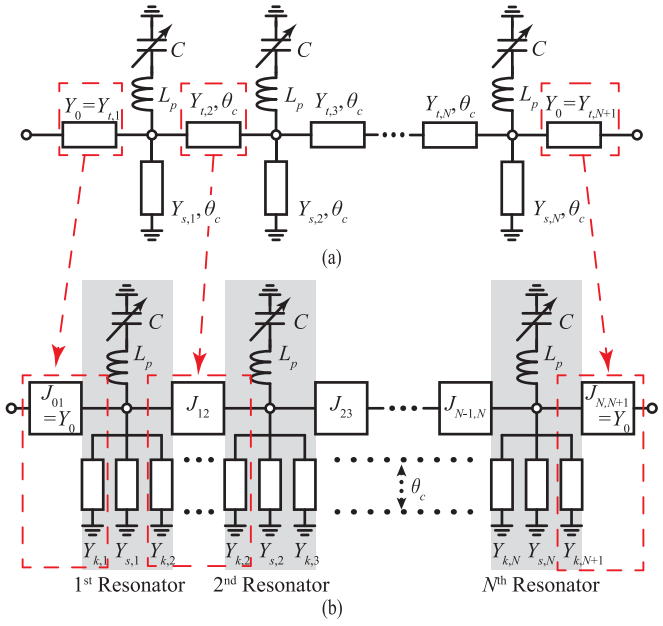

Fig. 1. Proposed N^{th}-order tunable filter (a) schematic, (b) its equivalent circuit based on J inverters and shunt resonators.

and fabricated. The experimental results show a very wide frequency tuning range of 62.8% at 2.22 GHz, in which the 3-dB bandwidth remains within 28.65±1.55% with a minimum insertion loss of 1.7 dB, and spurious suppression of below −40 dB up to as high as $3f_0$.

II. Design Theory of a Tunable Filter

Figure 1(a) shows the schematic of the proposed N^{th}-order filter, which consists of transmission lines, stubs, and variable capacitors. All transmission lines and stubs are shorter than a quarter-wavelength at the operating frequency f_c. All resonators are tuned with the same capacitance, allowing not only low-cost fabrication due to the use of identical varactors, but also simple tuning using a single bias control. A parasitic inductance L_p is associated with the varactors as well as junction between the pads and varactor package, etc.

The proposed equivalent circuit of the filter is shown in Fig. 1(b), where the transmission lines in the middle sections are modeled with a J inverter loaded with shunt stubs on both sides. The equivalence is shown in Fig. 2(a), which requires the following conditions [16]:

$$J_{i-1,i} = Y_{t,i}\csc\theta_c, \quad Y_{k,i} = Y_{t,i}. \qquad (i = 2, 3, \ldots, N). \quad (1)$$

However, if this equivalent model is adapted to the first and last transmission lines sections of Fig. 1(a), additional shunt capacitors are required to resonate the shunt stubs at the input and output ports. As in [17], [18], these capacitors are different from other capacitors. In this brief, to tune the resonator with identical varactors, the transmission lines at both ends are modeled in a nonconventional way, i.e., with a stub only on one side, as shown in Fig. 2(b). This can be done with the following conditions:

$$J_{i-1,i} = Y_{t,i}, \quad Y_{k,i} = Y_0 - J_{i-1,i}^2/Y_0. \quad (i = 1, N+1). \quad (2)$$

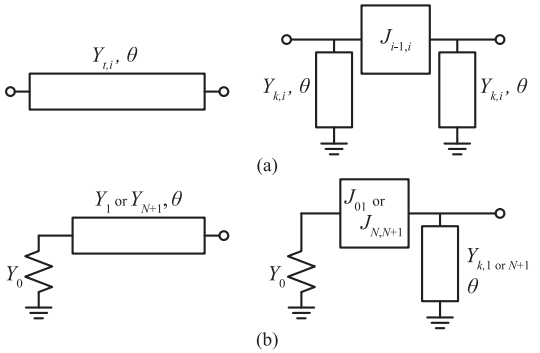

Fig. 2. The transmission line and its conventional equivalent circuit: (a) for transmission line section in the middle, (b) for transmission line section at both ends.

When the characteristic admittance of the transmission lines at both ends is equal to the system admittance, i.e., when $Y_{t,1} = Y_{t,N+1} = Y_0$, the J inverter values at both end become system admittance, i.e., $J_{01} = J_{N,N+1} = Y_0$. In addition, the first and last grounded stub on the equivalent circuit in Fig. 1(b), $Y_{k,1}$ and $Y_{k,N+1}$ may be removed since $Y_{k,1} = Y_{k,N+1} = 0$, which then indicates that the stubs are open circuited. It means that by utilizing different equivalent circuits and conditions for transmission line sections of the proposed filter in Fig. 1(a) depending on their locations, not only size reduction is achieved, but also with identical resonators. The latter allows frequency tuning with identical varactors, controlled by a single bias.

The resonators in Fig. 1(b) must resonate at the center frequency ω_c. Because C and L_p are identical in all resonators, the sum of the total admittance of all stubs and the series LC in each resonator must vanish, i.e.,

$$Y_{k,i} + Y_{s,i} + Y_{k,i+1} = \frac{\omega_c C}{1 - \omega_c^2 L_p C}\tan\theta_c, \qquad (3)$$

where $i = 1, 2, 3, \ldots, N$ with $Y_{k,1} = Y_{k,N+1} = 0$. This resonant condition clearly shows that the center frequency can be tuned by C, i.e., it can be increased by decreasing C, and vice versa.

Now that the complete equivalent conditions for the two circuits in Fig. 1 are established, the conventional filter synthesis method in [17] can be applied readily. From (1)-(3), the following design equations for the initial state are derived.

$$Y_{t,i} = Y_{k,i} = \frac{g_0 g_1}{\sqrt{g_{i-1}g_i}} Y_0 \sin\theta_0, \quad (i = 2, 3, \ldots, N-1) \quad (4)$$

$$C_0 = \frac{-b - \sqrt{b^2 - 4ac}}{2a}, \qquad (5)$$

where

$$a = \frac{2g_0 g_1}{\Delta_r} Y_0 \omega_0^4 L_p^2 + \omega_0^3 L_p(\theta_0 \csc^2\theta_0 \tan\theta_0 - 1),$$

$$b = -\frac{4g_0 g_1}{\Delta_r} Y_0 \omega_0^2 L_p - \omega_0(\theta_0 \csc^2\theta_0 \tan\theta_0 + 1),$$

$$c = \frac{2g_0 g_1}{\Delta_r} Y_0,$$

g_i is the prototype value, Δ_r is the fractional bandwidth, and f_0 is the center frequency of the initial state, i.e., when C=C_0,

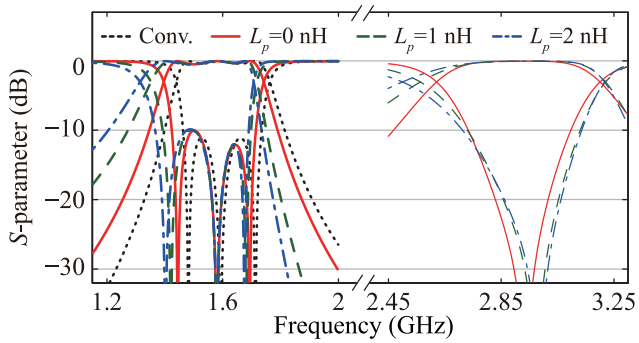

Fig. 3. Ideal simulation results of 3-pole single-band and proposed filters with θ_0=15° for various L_p.

and θ_0 is electrical length at f_0. The characteristic admittance of all stubs $Y_{s,i}$ (i=1, 2,..., N) can be calculated from (3)-(5). The other solution for C_0 is trivial because it yields negative characteristic impedances for the stubs.

While the characteristic admittances of the transmission line sections in (4) are invariant with respect to L_p, those of the stubs and C depend on L_p. As L_p increases, the right-hand side of (3) and $Y_{s,i}$ in the left-hand side decreases because $Y_{k,i}$ and $Y_{k,i+1}$ are determined by (4). This reduces the difference between the characteristic admittances of the stubs $Y_{s,i}$ and the transmission line sections $Y_{t,i}$. Therefore, the filter can be fabricated on a single substrate with uniform thickness, which is another great advantage compared to other filters that require transmission lines of with very wide range of characteristic impedances [18]. Because the proposed method is based on the conventional filter synthesis method that is based on inverters and resonators, the method is appropriate for narrow to moderate bandwidths. However, the characteristic impedances may be too high to implement for very narrow bandwidths.

Figure 3 shows the ideal response of the proposed filter with θ_0=15° at f_0=1.6 GHz where it is designed to have a 0.35-dB ripple level with a fractional bandwidth of Δ_r=18% in the initial state. For comparison, the ideal 3rd-order Chebyshev filter response at 1.6 GHz with a 0.35-dB ripple level and Δ_r=18% is also provided. The comparison shows good agreement between the two, validating the equivalence between the ideal filter and the proposed filter at the initial state.

Figure 3 also shows the performance of the filter when the center frequency f_c is tuned up to about 2.9 GHz assuming a maximum ratio of $C_{\text{ratio}}=C_0/C$ to 3.67 between the initial (C_0) and minimum capacitances, for various L_p. As the frequency is tuned, the ripple level is reduced and the location of the poles become closer. This is due to the changes in the filter prototype value to compensate the changes in the C and the electrical length θ_c in (4) and (5), due to the change in the operating frequency.

Figure 4 shows the calculated change in $\Delta_{3\text{-dB}}$ of the proposed filter, for the two states when the loaded capacitance $C=C_0/C_{\text{ratio}}$ is tuned from C_{ratio}=1 to 1.8 and 3.67 with respect to the parasitic reactance $\omega_0 L_p$ and electrical length θ_0, both at the initial state. These results can be utilized to estimate the changes in the 3-dB fractional bandwidth accurately as the frequency is tuned. The results show that the effect of $\omega_0 L_p$ on

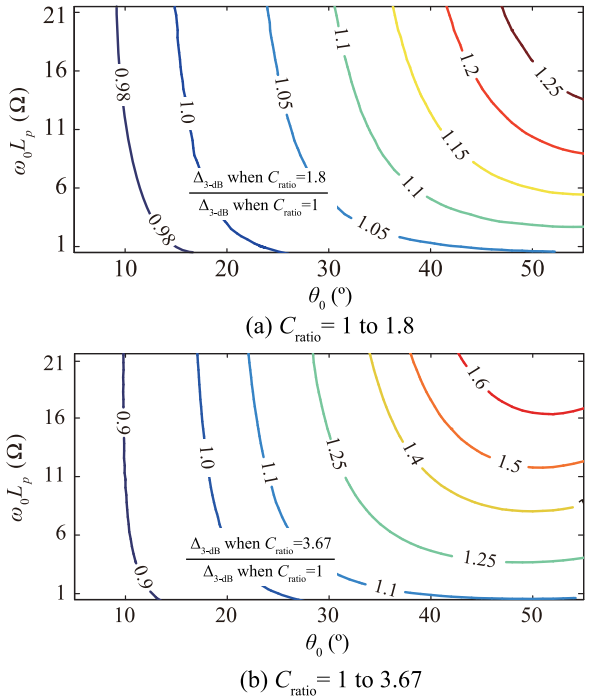

Fig. 4. Ratio of $\Delta_{3\text{-dB}}$ when (a) C_{ratio}=1.8 and (b) when C_{ratio}=3.67 with respect to $\omega_0 L_p$ and θ_0. The filter in initial state is a third-order filter with 0.35-dB ripple level and Δ_r=18%.

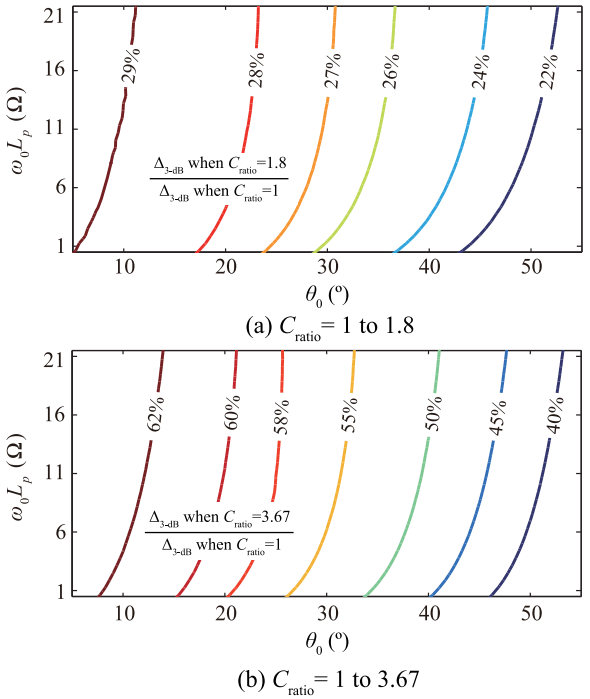

Fig. 5. Frequency tuning range when (a) C_{ratio}=1.8 and (b) when C_{ratio}=3.67 with respect to $\omega_0 L_p$ and θ_0. The filter in initial state is a third-order filter with 0.35-dB ripple level and Δ_r=18%.

the fractional bandwidth is different for a different θ_0, suggesting that the bandwidth can be maintained, reduced, or widened as it is tuned by selecting an appropriate θ_0. For instance, for $\omega_0 L_p$=15.1 Ω and θ_0=39°, the $\Delta_{3\text{-dB}}$ is 1.15 times wider than that of the initial state when the capacitance is tuned to 1/1.8

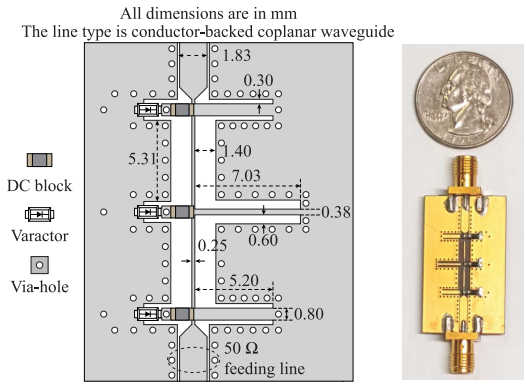

Fig. 6. (a) Layout and (b) photograph of the fabricated filter.

times of C_0, as shown in Fig. 4(a). Otherwise, if the initial electrical length is set to θ_0=16°, the fractional bandwidth can be maintained as the center frequency is tuned.

The comparison between Fig. 4(a) and (b) reveals that the change in the bandwidth becomes more sensitive to $\omega_0 L_p$ and θ_0 for a higher C_{ratio}. However, the electrical length that maintains the fractional bandwidth in both figures remains nearly the same, i.e., θ_0=16° and θ_0=17° with $\omega_0 L_p$=15.1 Ω, even when C_{ratio} is twice as large. This is a clear indication that when a filter is designed to maintain the fractional bandwidth at the initial and the last state, the filter also maintains the fractional bandwidth at the middle state. Further, when the goal is to expand the fractional bandwidth as the frequency is tuned, then a smaller miniaturization rate, or equivalently a longer θ_0 should be chosen.

Figure 5 shows the calculated frequency tuning range of the proposed filter when the loaded capacitance C=C_0/C_{ratio} is tuned from C_{ratio}=1 to 1.8 and 3.67. The results suggest that the parasitic inductance L_p have an effect on the center frequency in the tuned state, as seen previously in the ideal simulation results in Fig. 3. More importantly, a larger frequency tuning range can be achieved with a higher miniaturization rate, or equivalently a shorter θ_0, or by using varactors with a higher C_{ratio}.

Because the proposed tunable filter is based on reduced-length transmission lines, a very wide frequency tuning range is achieved since, theoretically, the filter can be tuned up to the point when the transmission line section becomes 90° and the loading capacitance C=0, i.e., f_c=f_0×90°/θ_0. Thus, the smaller the θ_0, the wider the frequency tuning range. Then, by designing the proposed filter to utilize the maximum range of the capacitance ratio of the varactor, which is limited in practice, based on the pre-calculated filter performance shown in Fig. 4 and Fig. 5, the proposed filter can provide a wide frequency tuning range with the designed bandwidth ratio. For instance, for $\omega_0 L_p$=15.1 Ω and C_{ratio}=3.67, θ_0=16° maintains a bandwidth ratio of virtually one, as the filter is tuned from 1.6 GHz to 3.0 GHz, which is a frequency tuning range of 61%.

Although not shown in here, the method can be utilized to develop a constant absolute-bandwidth filter. This can be done by converting the curves in Figs. 4 and 5 to absolute bandwidths. Finally, because the proposed filter is based on miniaturized transmission lines, it naturally exhibits a superior stopband response. This will be demonstrated in the next session.

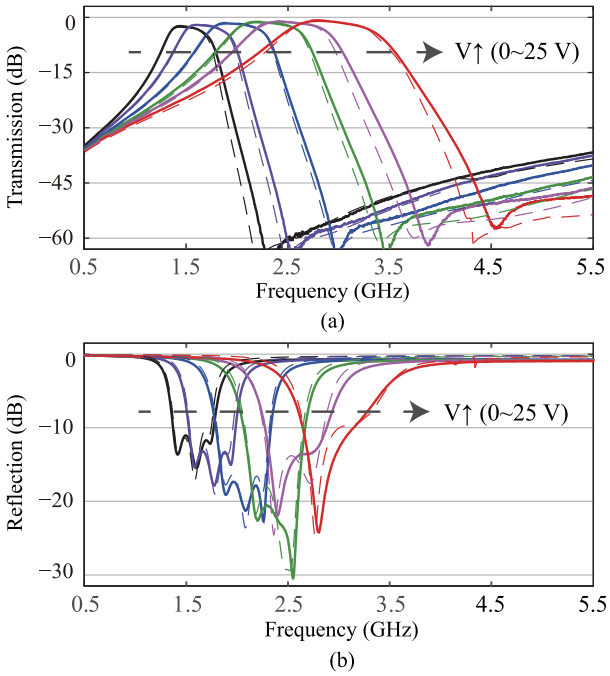

Fig. 7. Measured (thick) and simulated (thin) results: (a) Transmission S_{21} and (b) Reflection S_{11}.

III. Experimental Results

For experimental verification, a 3rd-order Chebyshev tunable filter is designed and fabricated. The filter is designed to have a ripple level of 0.35 dB with a fractional bandwidth of Δ_r=18% at f_0=1.5 GHz.

The design procedure can be summarized as follows. First, the filter specification for the lowest band is determined. Then, the design parameters are calculated from (3)-(5). When the varactors and therefore the maximum C_{ratio} are determined, design curves similar to those in Figs. 4 and 5 can be obtained. From these curves, the optimal θ_0 is determined depending on how the bandwidth is to vary as the filter is tuned. However, the parasitic inductance L_p is from the varactor and also from the full-wave simulated results of the junctions for an initial θ_0. Therefore, L_p may change with respect to θ_0 and then θ_0 has to be reselected. This step is iterated until all design goals converge. Although the procedure is shown for a 3rd-order filter, the method can be applied to higher order filters by solving (3)-(5) for an arbitrary N.

In this brief, Skyworks SMV1405 varactors are used. The capacitance tuning range C_{ratio}=3.67 is obtained experimentally when the bias is changed from 0 V to 25 V. The parasitic inductance L_p is set to 1.5 nH, which is also obtained experimentally. The final design parameters are θ_0=15°, $Z_{t,2}$=171.4 Ω, $Z_{s,1}$=71.1 Ω, $Z_{s,2}$=121.4 Ω, and C_0=3.49 pF. In this case, from Fig. 4(b) and Fig. 5(b), the filter is expected to maintain the $\Delta_{3\text{-dB}}$=24.9% from 1.5 GHz up to 2.82 GHz, which is a frequency tuning range of 61.5%.

The optimized layout and photograph of the fabricated filter are shown in Fig. 6. The filter is fabricated on a 1.28-mm-thick

TABLE I
SUMMARY AND COMPARISON OF THE FILTER PERFORMANCE

Reverse bias (V)	0	0.5	2	5	10	25
f_c (GHz)	1.52	1.69	1.99	2.29	2.52	2.91
3-dB FBW (%)	27.1	28.1	29.1	29.9	30.2	29.9
IL (dB)	3.2	2.8	2.4	2.1	2.0	1.7

Ref.	Frequency range GHz, (%)	FBW % (Ratio*)	Insertion Loss (dB)	Stopband†	Size ($\lambda_g \times \lambda_g$)
[5]	1.17-1.92 (48.5)	9.4-9.9 (1.05)	2.9-6.0	$2.2f_0$	0.25×0.2
[6]	2.19-2.55 (15.2)	6.2-6.8 (1.10)	2.8-4.9	$2.1f_0$	0.18×0.13
[7]	1.62-1.96 (19.0)	4.5-5.1 (1.13)	2.8-2.9	N/A	0.42×0.32
[9]	0.78-0.92 (16.5)	20-23 (1.15)	0.7-1.4	N/A	0.18×0.10
[11]	0.43-0.72 (50.4)	2.75-3.2 (1.16)	0.8-3.8	N/A	N/A
[12]	0.23-0.40 (56%)	2.5-2.6 (1.04)	5.6-9.2	$5.8f_0$	N/A
[13]	0.6-1.02 (51.4)	15.2-15.9 (1.04)	1.1-2.8	$2.0f_0$	0.19×0.19
[14]	0.97-1.53 (44.0%)	5.0-6.0‡ (1.20)	2.0-4.2	$1.8f_0$	0.10×0.09
Proposed	1.52-2.91 (62.8)	27.1-30.2 (1.11)	1.7-3.2	$3.0f_0$	0.11×0.08

∗: (Max. FBW)/(Min. FBW), ‡:1-dB bandwidth
†: The highest out of frequency that maintains $|S_{21}| <$ -40 dB.

Taconic RF-60A substrate with ε_r=6.15. The filter has a very compact size of $0.11\lambda_g \times 0.08\lambda_g$ (16.6×12.7 mm^2) at 1.52 GHz. In the fabricated filter, 33-pF SMD-type capacitors are used as DC blocks, and 10-MΩ resistors are used as RF chokes. The reverse bias to each varactor is from the bottom side through the via hole that connect the DC blocks on the bottom side of the substrate with the varactors on the top side of the substrate.

Figure 7 shows the responses measured using an E5071B VNA from Keysight, after achieving electronic calibration with an N4431A calibration module. The figure also show full-wave simulation results by HFSS. By increasing the bias voltage from 0 V to 25 V, the center frequency is tuned from 1.52 GHz to 2.91 GHz, which corresponds to a frequency tuning range of 62.8%. In this range, $\Delta_{3\text{-dB}}$ remains 28.7±1.6% while maintaining a reflection of less than −10 dB in the entire tuning range. The measured reflection of −10 dB corresponds very well with the designed ripple level of 0.35 dB, which can be reduced to improve the ripple level.

The out-of-band transmission is below −40 dB up to as high as $3f_0$ for the initial state, demonstrating its outstanding spurious suppression performance. The minor discrepancy between the measured and simulated bandwidths is due to the Q factor of the varactors, which decreases with the bias. For the proposed filter, the effects of Q factors on the insertion loss is similar as other filters [16]. The measured insertion loss is 3.2 dB in the initial state, and decreases to 1.7 dB at the highest band, which is comparable with those in [6] based on the same varactors. Table I summarizes the performance of the demonstrated filter, and compares it with previous tunable filters. Further improvement in the lower stopband can be achieved by introducing transmission zeros, for example, by loading stubs at both the input and output sides.

IV. CONCLUSION

A design method for a frequency-tunable filter is demonstrated. Because all resonators are designed to have the same capacitances, the filter can be tuned with identical varactors using a single bias control. Therefore, the structure and design procedure are simple, and low-cost fabrication is possible. Furthermore, the filter is based on reduced-length transmission lines that provide a compact size, wide frequency tuning range, and great out-of-band response. The demonstrated third-order Chebyshev filter is based on θ_0=15° lines, resulting in a very small size of $0.11\lambda_g \times 0.8\lambda_g$. The center frequency is tuned from 1.52 to 2.91 GHz, which is a 62.8% bandwidth. In this range, the spurious response remained below −40 dB and up to as high as $3f_0$, where f_0 is the center frequency, while maintaining a fractional bandwidth of 28.7±1.6%. Although a constant absolute-bandwidth filter can be designed with the proposed method, the tuning range is relatively narrow. This can be overcome by modifying transmission line section to provide constant inverter value as the frequency is tuned, which remains as future work.

REFERENCES

[1] G. Sung, "Compact dual-band bandpass filter using U-shaped stepped-impedance resonators with parallel coupled structures," *J. Electromagn. Eng. Sci.*, vol. 18, no. 2, pp. 73–77, Apr. 2018.

[2] W. Feng, Y. Zhang, and W. Che, "Tunable dual-band filter and diplexer based on folded open loop ring resonators," *IEEE Trans. Circuits Syst. II, Exp. Briefs*, vol. 64, no. 9, pp. 1047–1051, Sep. 2017.

[3] M. Yuceer, "A reconfigurable microwave combline filter," *IEEE Trans. Circuits Syst. II, Exp. Briefs*, vol. 63, no. 1, pp. 84–88, Jan. 2016.

[4] D.-S. Kim, D.-H. Kim, and S.-W. Yun, "Design of an active tunable bandpass filter for spectrum sensing application in the TVWS band," *J. Electromagn. Eng. Sci.*, vol. 17, no. 1, pp. 34–38, Jan. 2017.

[5] Y. C. Li and Q. Xue, "Tunable balanced bandpass filter with constant bandwidth and high common-mode suppression," *IEEE Trans. Microw. Theory Techn.*, vol. 59, no. 10, pp. 2452–2460, Oct. 2011.

[6] Q. Xiang, Q. Feng, X. Huang, and D. Jia, "Electrical tunable microstrip LC bandpass filters with constant bandwidth," *IEEE Trans. Microw. Theory Techn.*, vol. 61, no. 3, pp. 1124–1130, Mar. 2013.

[7] H.-Y. Tsai, T.-Y. Huang, and R.-B. Wu, "Varactor-tuned compact dual-mode tunable filter with constant passband characteristics," *IEEE Trans. Compon. Packag. Manuf. Technol.*, vol. 6, no. 9, pp. 1399–1407, Sep. 2016.

[8] W.-J. Zhou and J.-X. Chen, "High-selectivity tunable balanced bandpass filter with constant absolute bandwidth," *IEEE Trans. Circuits Syst. II, Exp. Briefs*, vol. 64, no. 8, pp. 917–921, Aug. 2017.

[9] G. Suo *et al.*, "Low loss tunable superconducting dual-mode filter at L-band using semiconductor varactors," *IEEE Microw. Wireless Compon. Lett.*, vol. 24, no. 3, pp. 170–172, Mar. 2014.

[10] A. Anand, J. Small, D. Peroulis, and X. Liu, "Theory and design of octave tunable filters with lumped tuning elements," *IEEE Trans. Microw. Theory Techn.*, vol. 61, no. 12, pp. 4353–4364, Dec. 2013.

[11] C. Li *et al.*, "A tunable high temperature superconducting bandpass filter realized using semiconductor varactors," *IEEE Trans. Appl. Supercond.*, vol. 24, no. 5, pp. 1–5, Oct. 2014.

[12] A. Zakharov, S. Rozenko, and M. Ilchenko, "Varactor-tuned microstrip bandpass filter with loop hairpin and combline resonators," *IEEE Trans. Circuits Syst. II, Exp. Briefs*, vol. 66, no. 6, pp. 953–957, Jun. 2019.

[13] W. Qin, J. Cai, Y.-L. Li, and J.-X. Chen, "Wideband tunable bandpass filter using optimized varactor-loaded SIRs," *IEEE Microw. Wireless Compon. Lett.*, vol. 27, no. 9, pp. 812–814, Sep. 2017.

[14] L. Gao and G. M. Rebeiz, "A 0.97–1.53-GHz tunable four-pole bandpass filter with four transmission zeroes," *IEEE Microw. Wireless Compon. Lett.*, vol. 29, no. 3, pp. 195–197, Mar. 2019.

[15] M. Ohira, S. Hashimoto, Z. Ma, and X. Wang, "Coupling-matrix-based systematic design of single-DC-bias-controlled microstrip higher order tunable bandpass filters with constant absolute bandwidth and transmission zeros," *IEEE Trans. Microw. Theory Techn.*, vol. 67, no. 1, pp. 118–128, Jan. 2019.

[16] T. Lim, B.-W. Min, and Y. Lee, "Miniaturisation method for coupled-line bandpass filters with identical and minimal number of reactive elements," *IET Microw. Antennas Propag.*, vol. 8, no. 14, pp. 1192–1197, Nov. 2014.

[17] S. Lee and Y. Lee, "Generalized miniaturization method for coupled-Line bandpass filters by reactive loading," *IEEE Trans. Microw. Theory Techn.*, vol. 58, no. 9, pp. 2383–2391, Sep. 2010.

[18] A. Miller and J. Hong, "Cascaded coupled line filter with reconfigurable bandwidths using LCP multilayer circuit technology," *IEEE Trans. Microw. Theory Techn.*, vol. 60, no. 6, pp. 1577–1586, Jun. 2012.